Flume and field-based calibration of surrogate sensors for monitoring bedload transport

Mao L.[1*], Carrillo R.[1], Escauriaza C.[2,3], Iroume A.[4]

[1]Pontificia Universidad Católica de Chile, Department of Ecosystems and Environments, Santiago, Chile

[2]Pontificia Universidad Católica de Chile, Department of Hydraulic and Environmental Engineering, Santiago, Chile

[3]Pontificia Universidad Católica de Chile, National Research Center for Integrated Natural Disaster Management, Santiago, Chile

[4]Universidad Austral de Chile, Faculty of Forest Sciences and Natural Resources, Valdivia, Chile

[*] Corresponding Author. Pontificia Universidad Católica de Chile, Department of Ecosystems and Environments, Av. Vicuña Mackenna 4860, Macul, Santiago, Chile. Email: lmao@uc.cl

Abstract

Bedload transport assessment is important for geomorphological, engineering, and ecological studies of gravel-bed rivers. Bedload can be monitored at experimental stations that require expensive maintenance, or using portable traps, which allows measuring instantaneous transport rates, but at a single point and at high costs and operational risks. The need of measuring continuously bedload intensity and dynamics has therefore increased the use and enhancement of surrogate methods. This paper reports on a set of flume experiments on which a Japanese acoustic pipe and an impact

plate have been tested using four well-sorted and three poorly-sorted sediment mixtures. Additional data were collected in a glacierized high-gradient Andean stream (Estero Morales) using a portable Bunte-type bedload sampler. Results show that the data provided by the acoustic pipe (which is amplified on6 channels having different gains) can be calibrated for both the grain size and the intensity of transported sediments coarser than 9 mm (R^2= 0.93 and 0.88, respectively). Even if the flume-based calibration is very robust, the upscale to the field is more challenging, and the bedload intensity could be predicted better than the grain-size of transported sediments (R^2= 0.61 and 0.43, respectively). The inexpensive impact plate equipped with accelerometer could be calibrated for bedload intensity quite well in the flume but only poorly in the field (R^2= 0.16), and could not provide information on the size of transported sediments.

Keywords: Transported grain-size, impact plate, acoustic pipe, Bunte-type sampler, mountain streams, Andes.

1. Introduction

Quantifying coarse sediment transport is of crucial importance for civil engineers, geomorphologists, river ecologists and managers (e.g. Rickenmann andKoschni, 2010), as bedload determines river morphodynamics, and type and persistence of riverine habitats. Equations for bedload prediction are usually derived from flume experiments, and tend to overestimate the actual sediment transport (e.g. Barry et al., 2004; Vazquez-Tarrioand Duarte, 2015), especially when applied to ordinary floods (D'Agostinoand Lenzi, 1999) and under conditions of limited sediment supply (Recking, 2012). On the other hand, field bedload monitoring is notoriously difficult and expensive. Continuous measurements of bedload fluxes can be achieved in experimental stations using vortex-

type (Tacconi and Billi, 1987), Reid-type slot samplers (Lucia et al, 2013), or stations in which bedload and water fluxes can be separated (Bogen and Møen, 2003; Lenzi et al, 2004, Rickenmann et al., 2012), but are expensive to maintain and observations are limited to a single cross-section. Field samplings can be achieved using portable basket traps, mainly Helley-Smith (Emmett, 1980) and Bunte-type traps (Bunte et al., 2004, 2007) that can be handled from bridges, boats, or wading the channel bed. Although traps allow to monitor the size and intensity of sediment transport, there are issues related with the limited duration of bedload sampling (Bunte and Abt, 2005), size of traps, and disturbances on the bed produced by the same samplers (Vericat et al., 2006). Also, samples can be taken only occasionally, and sampling during flood events is challenging and dangerous. These limitations are especially evident in high-gradient mountain streams, where flood events tend to be short and unpredictable. More importantly, mountain streams feature coarse grain sizes, uneven bed surface, high temporal variability of bedload transport, and changes in sediment supply conditions (Comiti and Mao, 2012; Rickenmann et al., 2012), all of which makes continuous measurements with indirect methods very appealing.

Bedload can be monitored indirectly using morphological methods or methods based on virtual velocity of tracers (Liebaultand Laronne, 2008), or with a variety of surrogate devices such as piezoelectric sensors (e.g. Rickenmann and McArdell, 2007), acoustic sensors (Rennie and Church, 2010), acousticpipe sensors (Mizuyama et al., 2003, 2010a,b), hydrophones (Geay, 2013),geophones (Rickenmann et al., 2014; Hilldale et al., 2014), and other sensors fixed beneath steel plates. Comprehensive reviews of the techniques and devicesare providedfor instance by Gray et al. (2010) and Rickenmann et al. (2012, 2014).

Even if uncalibrated, bedload sensors can provide precious indications on the beginning and end of bedload transport (Turowski et al., 2011), dynamics of bedload during flood events (BeylichandLaute, 2014; Mao et al., 2014), and sediment supply conditions (BeylichandLaute, 2014). However, there is a growing body of literature devoted at calibrating surrogate sensors versus actual bedload transport rates and size measured either in the laboratory or in the field. Rickenmann et al. (2014) calibrated Swiss plate geophones using field data collected using samplers or traps in five mountain streams, and reported that the number of collected impulses correlated with bedload mass of coarse grains, further observing that the number of impulses per bedload mass depends on the velocity of the flow, mode of sediment movements, and size of transported sediments.BeylichandLaute (2014) calibrated an impact sensor equipped with an accelerometer using data collected over a range of field sites and conditions and in a series of flume experiments, reporting that the raw data provided by the sensors could be calibrated for bedload intensities of sediments coarser than 11.3 mm. Working on the whole range of acoustic signals provided by a geophone, Tsakaris et al. (2014) were able to calibrate in a flume the transport intensities and to differentiate impacts produced by rolling and saltating sediments.More recently, Barriere et al. (2015) developed a sophisticated signal processing technique for analysing the amplitude and frequency of each impact registered by a piezoelectric hydrophone, which allowed predicting the median grain size of transported sediments. Using Bunte-type samples taken on a glacierized mountain river, Dell'Agnese et al. (2014) were able to calibrate the bedload transport rates analysing only raw data recorded with a Japanese acoustic pipe.

Overall, to date there have been only few attempts of calibrating surrogate devices in both field and flume conditions, and very little examples of calibration of more than one

sensor at a time. The main objective of this study is to calibrate a Japanese acousticpipe and a simple impact plate encapsulating an accelerometer in order to obtain information on intensity and size of transported sediments. The study is based on a series of flume experiments using sediments ranging from 5 to 40 mm, and on Bunte-type samples taken in a high-gradient, boulder-bed stream of the Andes. We analysed the number of impulses exceeding a certain threshold as provided by the sensors, in order to develop a robust and practicalway of deriving the grain size and the rate of coarse sediment transport.

2. Materials and Methods

A series of flume experiments using well- and poorly-sorted sediment mixture were carried out to test the performance of a Japanese acoustic pipe (Mizuyama et al., 2010a,b) and a bedload impact plate (Richardson et al., 2003), which were then installed in a highgradient stream where Bunte-type bedload samplings were taken.

2.1.Tested devices

In this study we used a 0.5 m long acoustic pipe sensor (diameter 4.8 cm), manufactured by Hydrotech Company (Japan; Mizuyama et al., 2003, 2010a, 2010b). The Japanese acoustic pipe sensor is an empty steel pipe with a microphone inside which detects the acoustic vibrations induced by particles hitting the device. Acoustic pressure waves induced by moving particles hitting the pipe generate a signal amplified by a pre-amplifier and then transmitted to a converter. The converter generates a voltage which is processed through a 6-channel band-path filter (with channel 1 and channel 6 corresponding to the highest and lowest sensitivities, respectively). The band-path filters have lower (2.5 V) and upper (5 V) thresholds, hence an pulse is generated when the output of a channel exceeds 2.5 V. Each channel has a gain of 4 relative to the

121 previous, lesser voltage-output channel, e.g. the 6-channel voltage exiting the
122 converter's amplifier for a 10 mV signal is: channel 6 (×1) = 10 mV; channel 5 (×4)
123 =40mV; channel 4 (×16)=160mV; channel 3 (×64)=640; channel 2 (×256)=2.56 V;
124 channel 1 (×1016)= 10.16 V (for more details, see Mizuyama et al., 2010a; Dell'Agnese
125 et al., 2014; Mao et al., 2014).The converted signal is then processed by an 8-channel
126 interval timer attached to a datalogger, sampling the signal at a frequency of 5 Hz.

127 A simple bedload impact plate (Richardson et al., 2003) was tested along with the
128 acoustic pipe. The device is composed by a slightly convex stainless steel plate (130
129 mm x 150 mm x 6 mm) under which a 60 mm diameter steel cylinder encloses an
130 accelerometer. A count input data logger connected to the accelerometer allows to
131 register the cumulated number of impacts sensed at a certain time interval. The loggers
132 can record up to 255 impacts within a given time interval, up to 5 impacts per second.

133 *2.2.Flume experiments*

134 A series of experiments were carried out in a 10 m-long, 0.4 m-wide tilting flume at the
135 Department of Hydraulic and Environmental Engineering of the Pontificia Universidad
136 Católica de Chile. To reduce inlet and backwater effects, 1 m and 1.5 m-long artificially
137 roughened bed sections were placed at both the upstream and downstream ends of the
138 flume, respectively. The downstream adjustable weir was laid flat to allow the flow
139 depth to adjust naturally. Water levelwas measured at8locations along the flume every
140 30 minutes. Seven different sediment mixtures were used in the experiments (Figure 1).
141 Four mixtures were relatively well sorted (standard deviation of the grain size curves σ
142 always < 1.2), and the D_{50} was of 5.6, 13.0, 24.6, and 35.9 mm, respectively. Thesewell
143 sorted sediments were then mixed in order to produce poorly sorted distributions with
144 higher standard deviation and intermediate D_{50}. Thus, the two finer well sorted
145 sediments were combined to produce a mixture with σ = 1.7 and D_{50} = 9.0 mm, and the

146 two coarser well sorted sediments were combined to produce a mixture with $\sigma = 1.4$ and
147 $D_{50} = 27.3$ mm. Also, the four well sorted sediments were combined to obtain a very
148 poorly sorted grain size distribution curve with $\sigma = 2.5$ and $D_{50} = 15.2$ mm.

149 Bed load traps with 1 mm metal mesh were used to collect sediments at the downstream
150 end of the flume. Sediment traps located at the downstream end of the flume were
151 changed when approximately half full of sediments, and replaced by an empty one
152 without stopping the pumps. Sediment collected with the trap was quickly weighted and
153 recirculated manually into the fixed artificially roughened bed sections at the upstream
154 end of the flume. Sediment was recirculated at intervals ranging from 1 to 40 min
155 depending on the bed load transport rate. However, at least 200 g of sediment was
156 collected prior to emptying the traps. Because the standard deviation of the well sorted
157 sediments sediment mixtures was very small, it was assumed that the grain size of the
158 transported material was equal to the grain size of the mixture in the flume. For the
159 poorly sorted sediment mixture, a sample of the transported material collected on the
160 trap was taken at each trap recirculating, and quickly dried and sieved in order to obtain
161 the grain sizes of the transported sediments.

162 A series of runswere carried out for each grain size distribution curve, varying both
163 discharge and channel slope in order to produce a wide range of sediment transport
164 intensities(dimensionless shear stress ranging from approximately 0.06 to 0.1 for all
165 grain mixtures). Transport rates were calculated in g m^{-1} s^{-1} using the dried weight of
166 sediments collected at each trap changeover, the interval during which the trap collected
167 sediments, and the width of the flume. Transport rates spanned four orders of
168 magnitude, ranging from 0.08 to 453.44 g m^{-1} s^{-1}. Overall, 400 and 540 measurements
169 of sediment transport rates were taken using the well sorted and poorly sorted mixtures,
170 respectively.

On the fixed bed sections at the downstream end of the flume, just 50 cm upstream from the sediment trap, the 0.5 m long acoustic pipe sensor was fixed transversally to the flume length (Figure 2a), with half of its diameter exposed to the flow as suggested by the manufacturer. The number of impulses for each channel was recorded at 10 seconds interval in the datalogger. In order to calibrate the device using the amount and size of sediments collected at each recirculation, the number of impulses registered for each channel was summed over the duration of each sediment collection.Also, two bedload impact plates were installed on the fixed bed section just 20 cm upstream from the acoustic pipe, 5 cm apart from one another along the flume (Figure 2a). Data was collected at 10 second interval in order to avoid data saturation on the datalogger (i.e. occurrence of more than 255 impacts in each registering interval)even at the highest transport rates.

2.3.Field data collection

One acoustic pipe and one impact plate were installed in September 2014 in a high-gradient stream of the Chilean Andes called Estero Morales. The basin (27 km^2) ranges from 1850 m a.s.l. to 3815 m a.s.l., and hosts various littleglaciers, some uncovered and some covered by debris, with an overall current extent of 1.8 km^2 (Infante Fabres, 2009; Mao and Carrillo,submitted). Runoff is dominated by snowmelt in late spring (from late September to November),and glacier melt from December to March, providing a long season of daily fluctuations of discharge with coarse sediments being transported every day at different rates. In its lower part, just upstream of the confluence with the El Volcan River, the stream cuts into glacier deposits and it is confined and steep (0.14 m m^{-1}), featuring coarse sediments (D_{16} = 20.2 mm; D_{50} =59.1 mm; D_{84} = 317.5 mm; D_{90} = 448.1 mm)and a cascade/step-pool morphology.

195 The Japanese acoustic pipe sensor used in the flume (0.5 m long; diameter of 4.8 cm)
196 was mounted in a log installed transversally in the channel bed (Figure 2b), in a cross
197 section approximately 7 m wide. A slot waspreviously carved into the log to host half
198 the diameter of the steel pipe as done before (e.g. Dell'Agnese et al., 2014; Mao et al.,
199 2014). The log created a step of approximately its diameter (0.5 m) downstream, and
200 this prevented sediments to accumulate above the sensor. The datalogger and solar
201 panel system to supply the battery were installed in a boulder in the channel
202 bank.Impulses for the 6 amplification channels was registered at 1 minute interval. The
203 impact plate was installed in a 500 mm x 500 mm x 300 mm concrete box placed flush
204 with the bed surface 1 m upstream from the acoustic pipe. The sensor was set to record
205 the number of pings in successive 1 minute intervals.

206 Bedload field data for calibrating the acoustic pipe and the impact plate were collected
207 using a 30 cm wide Bunte-type trap (Bunte et al., 2004, 2007).Overall, 193 samples
208 were taken at the same location where the pipe and plate were installed, at a range of
209 discharge varying from 1 to 3 $m^3 s^{-1}$. The trap was placed just downstream of the impact
210 plate, but upstream of the Japanese pipe.Samples were taken from January to March
211 2015 for intervals ranging from 1 minute to 2 hours depending on the transport rate,
212 which ranged between 0.001 and 1851.9 g $m^{-1} s^{-1}$. The sediment collected in the traps
213 was dried and sieved in the laboratory. The grain size distribution of the bedload
214 samples was then calculated to obtain the significant percentiles (D_{16}, D_{50}, and D_{84}) and
215 the standard deviation of the mixture (σ) was derived as the root of the ratio between
216 D_{84} and D_{16}. Because the mesh of the Bunte traps was slightly larger than 3mm we
217 assume that the trap was able to capture sand with unclear efficiency, and then the grain
218 size distribution curves were all truncated at 4 mm. As done with the data collected in
219 the flume, the impulses generated by the acoustic pipe and the impact plate were

220 cumulated foreach sampling period, and then expressed as number of impulses per
221 second.

222

223 ## 3. Results

224 ### *3.1.Relationships between impulses and bedload transport rates*

225 The acoustic pipe sensor collects impulses due to sediment impacts in 6channels (i.e. 1
226 to 6, from the most to the less sensitive, respectively). The relationships between the
227 number of impulses (per minute and per meter of sensor length) registered by each
228 channel and sediment transport rate are shown in Figure 3. It appears that the number of
229 impulses increases with the intensity of sediment transport. Also, Figure 3 shows that
230 for the most sensitive channels (e.g. channels 1 to 3), atcertain transport intensity a
231 coarser mixture produces less impulses than a finer mixture. For example, at a transport
232 intensity of 10 g m^{-1} s^{-1}, channel 1 registered 0.3 and 10 impulses m^{-1} s^{-1} for mixtures
233 with D_{50} equal to 35.9 and 5.6 mm, respectively. Indeed, for each channel the
234 coefficient of the power-law regressions between transport and impact intensities
235 decrease consistently from the coarser to the finer mixture (Table 1). Also, for each
236 mixture, the coefficient of the power law regressions decreases for the more sensitive
237 channels, whereas the slope tends to increase (Table 1). It seems worth noting also that
238 the regression's coefficients change considerably among grain sizes, especially for the
239 more sensitive channels (e.g. channels 1 to 4). In fact, the coefficient of the regressions
240 derived using channel 2 for example are remarkably different if comparing the coarser
241 (WS = 35.9 mm) and the finer (WS = 5.6 mm) mixtures, being equal to 90.811 and
242 0.107, respectively (Table 1). Instead, the coefficients are comparable if values derived
243 from data collected in channel 5 are taken into account, being equal to 276.7 and 287.5,
244 respectively. Due to this effect, the regression curvesare more spaced for the more

245 sensitive channels (e.g. coefficients for channel 1 ranging from 50.9 to 0.031), than for
246 less sensitive channels (e.g. coefficients for channel 6 ranging from 349.7 to 184.4).

247 Data collected in the Estero Morales is plotted in Figure 3 as well, showing that for
248 channel 6 the intensity of impulses increases with sediment transport at a rate
249 comparable with what observed in the laboratory. For instance, the coefficient is around
250 381.6, similar to what was obtained for the coarsest mixture in the flume (349.7 for WS
251 = 35.9 mm). Instead, the slope of the regressions obtained with the Estero Morales data
252 increases for the more sensitive channels, and for channel 1 is virtually negative,
253 indicating that the number of data registered by the pipe sensor is insensitive to the
254 actual intensity of sediment transport.

255 *3.2.Relationships between impulses and the size of the transported sediment*

256 Data plotted in Figure 3 indicates that the acoustic pipe registersmore impulses at higher
257 transport rates. However, the regressions can be substantially different depending on the
258 grain size of the transported sediments. As a consequence, the grain size of the
259 transported material needs to be known in order to apply the correct regression and
260 relate impulses with transport rates. However, if the rates of impulses collected by the
261 6different channels are plotted one versus the others, some interesting patterns appear.
262 Figure 4 shows that if channels 1 and 3 are compared, data obtained for the coarsest
263 mixture plots along the line of equality, whereas finer grain sizes plots above the line of
264 equality suggesting that, as expected, more impulses are registered in the more sensitive
265 channel. This pattern is similar if impulses collected by more insensitive channels are
266 compared, and on each graph of Figure 4 it appears that different grain size mixture
267 tends to plot differently. The slope of each regression obtained combining all available
268 channels for all grain sizes have been analysed, and the pairs that allowed to better
269 discriminate between grain sizes are those plotted on Figure 4. A non-linear, power-law

regression was fitted, in order to obtain the grain size of transported sediments (D_{16}, D_{50}, and D_{84}) from the relationships between intensities of impulses registered for channels of different sensitivity:

$$D_{xx} = a\left(\frac{I_{s\_c1}}{I_{s\_c3}}\right)^{b}\left(\frac{I_{s\_c2}}{I_{s\_c4}}\right)^{c}\left(\frac{I_{s\_c3}}{I_{s\_c5}}\right)^{d}\left(\frac{I_{s\_c4}}{I_{s\_c6}}\right)^{e} \quad \text{Eq. 1}$$

where intensities (I_s) for each channel (from channel 1 $_{c1}$to channel 6 $_{c6}$) were used. The coefficient (a)and exponents (b, c, d, and e) of the regressions calculated for well sorted, poorly sorted, field data, and the whole database are reported on Table 2. The coefficients of determination obtained in the flume are very high, and are higher for the D_{50} than for finer or coarser fractions. Also, surprisingly, the coefficients of determination derived using poorly-sorted mixture are slightly higher than those obtained using well-sorted mixtures. As expected, the regressions calculated using data collected in the field are weaker (e.g. R^2 = 0.47 for the D_{50}). However, if the whole dataset is used, the R^2 of the regression needed to obtain the D_{50} is around 0.65, and all parameters are significant. As shown in Figure 5, the D_{50} of well-sorted mixtures can be predicted fairly well for mixture coarser than 10mm. In fact, for the finer mixture (D_{50} = 5.6 mm), Eq. 1 is not able to predict the median size of transported particles. This is due to the fact that grains are so small that less sensitive channels (e.g. 4 and 5) are rarely activated, as can be seen in Figure 3 and 4 as well. The regression derived for poorly-sorted mixture is also effective in predicting the D_{50} of transported sediments, for a size ranging from 10 to 40 mm. If only data collected in the field are used to derive the regression, the scatter becomes considerable (Figure 5), with a clear tendency of overestimating fine median grain sizes (< 10 mm), and underestimating the D_{50} of transported sediments coarser than 50 mm. Indeed, median grain sizes as coarse as 100 mm are underestimated by half (Figure 5). When all data are used to derive a regression

to estimate D_{50} for a range of grains ranging from 5 to 110 mm, Figure 5 confirms that sediments coarser than 40 mm tends to be strongly underestimated in size.

Apart from showing that the ratio between impulses registered by different channels plots differently depending on the grain size, Figure 4 allows appreciating that well- and poorly-sorted mixtures plot differently. Similarly to what is presented above, the slope of each regression obtained combining all available channels for all grain sizes have been analysed in order to obtain the standard deviation (σ) from the relationships between intensities of impulses registered for channels of different sensitivity, and the best non-linear regression was fitted, obtaining the following empirical power-law regression equation:

$$\sigma = a\left(\frac{I_{s\_c2}}{I_{s\_c4}}\right)^{b}\left(\frac{I_{s\_c3}}{I_{s\_c5}}\right)^{c}\left(\frac{I_{s\_c4}}{I_{s\_c6}}\right)^{d} \quad \text{Eq.2}$$

The coefficient (a) and exponents (b, c, and d) of the regressions obtained for well sorted, poorly sorted, field data, and the whole database are reported on Table 3. The R^2 of regressions obtained in the flume are fairly high, but its performance is low for the data collected in the Estero Morales ($R^2 = 0.28$). If the whole dataset is used, the R^2 of the regression needed to obtain σ is around 0.42.

3.3.Predicting bedload transport rates using the Japanese acoustic pipe

Figure 3 and Table 1 suggest that the rate of bedload transport (q_s, in g m^{-1} s^{-1}) could be predicted fairly well from the intensity of impulses collected by the acoustic pipe, provided that the grain size of the transported sediments is known. Because the grain size of the transported material could be derived from exploring the ratio between impacts registered for channels of different sensitivity, the best-fit non-linear equations

were fitfor regressions including the grain size of transported sediments (Eq. 3) andalso the standard deviation of transported mixture (Eq. 4):

$$q_s = aD_{50}{}^b I_{s\_c3}{}^c \left(\frac{I_{s\_c2}}{I_{s\_c5}}\right)^d \quad \text{Eq. 3}$$

$$q_s = aD_{50}{}^b I_{s\_c3}{}^c \left(\frac{I_{s\_c2}}{I_{s\_c5}}\right)^d \sigma^e \quad \text{Eq. 4}$$

The coefficients and exponents of the regressions obtained for well sorted, poorly sorted, field data, and the whole database are reported on Table 4. It appears that the empirical equations have high coefficient of determination if derived using data obtained in the flume, whereas if the dataset is expanded to include field data the performance of the regressions reduces (Figure 6). As expected, regressions feature higher coefficients of determination if the observed rather than the predicted values of transported grain sizes (D_{50} and σ) are used. Of course, if no samples are taken in the field, D_{50} and σ need to be calculated (using Eq. 1 and 2, respectively) in order to assess the intensity of sediment transport. Table 4 and Figure 6 show that the quality of the regression equationsimproves slightly if the standard deviation of the transported sediments is included. For instance, using all flume data the R^2 increases from 0.89 to 0.92 if observed values of grain sizes are considered, and from 0.87 to 0.88 if the predicted values of grain sizes are used in the regressions. If no direct field observation of transported grain size is available (which is the usual situation), data provided by the pipe acoustic sensor could be converted to actual bedload intensity using an empirical regression with $R^2 = 0.61$. Figure 6 e and f show that the inclusion of σ in the equation does not provide a better prediction of bedload rate, and that the actual transport rate is likely to be underestimated at the lower rates, whereas better predictions are expected at the highest bedload transport rates.

3.4.Relationships between impulses collected by the impact plate and bedload transport rates

The impact plate, whichrecordsvibrations due to impactsin a single channel, collects higher number of impulses at higher sediment transport rates. Figure 7shows that the slope of this relationship is fairly similar andspan from 1 to 2 approximately for the range of grain sizes explored in the flume experiments (Table 5). Instead, the coefficient of the power-law regressions increases for the coarser fractions, similarly to what is observedfor the acoustic pipe. Even if higher impulses are registered at the higher bedload intensities, the regression obtained from the field data is quite weak ($R^2 = 0.16$, Table 5).

4. Discussion

The results presented in this paper show that the Japanese acoustic pipe has the potential of being calibrated for grain size and transport intensity if all the6channels of different sensitivity at which it collects data are used. Because the size of transported material can strongly influence the relationship between impulses and transport rates, inferring the grain size from the same collected signal is critical for a successful calibration. Results from the flume experiments reveals that the grain size of transported material can be assessed by relating impulses registered on different channels. Previous flume calibrations of the same sensors showed that the number of pulses recorded by the pipe depends on the length of the pipe, the location on which the grain impacts on the pipe, the sensitivity of the microphone, and the size of grains (Mizuyama et al. 2010a). In the present study, the same pipe (0.5 m long) has been used in the flume and the field application. Mizuyama et al. (2010a) also found that impacts of particles as small as 4

363 mm could not be well detected by the sensor, and suggest a lower threshold of 8 mm for
364 bedload estimation using this device. Our results support this evidence in the way that,
365 not registering impulses on less sensitive channels,it was not possible to calculate
366 reasonably well the grain size of the finer mixture used in the flume runs (5.6 mm).
367 Therefore, even if less sensitive channels could still detect impacts produced by the
368 transport of this fine gravel particles (as in Mizuyama et al. 2010b), our calibration
369 results are applicable only for particles coarser than 9 mm.

370 Evidence from the field bedload sampling suggests a lower threshold of around 6 mm,
371 which coincides with what was reported by Dell'Agnese et al., (2014) from Bunte-type
372 bedload sampling in the Saldur River, a stream comparable to the Estero Morales in
373 terms of slope (0.05 and 0.1 mm^{-1}, respectively), grain size (D_{84} = 304 and 317 mm,
374 respectively), and basinarea (18.6 and 27 km^2, respectively).As to the estimation of the
375 size of transported sediments from the collected impulses data, evidences from the
376 flume experiments are encouraging, as the D_{50}can be accuratelypredicted. However,
377 field calibration is rather poor and this could be due to the transport of particles of
378 different sizes and shapes, mode of transport (rolling vs. saltation), but probably mostly
379 to the saturation of signals of the higher sensitivity channels (1 and 2), which does not
380 allow to calibrate well a regression like Eq. 1. Indeed, the saturation of high sensitive
381 channels of Japanese acoustic pipe even during low transport rates has been also
382 previously reported by Mizuyama et al. (2010b) and Dell'Agnese et al. (2014). This
383 issue could probably be overcome by processing directly the raw data (similarly to what
384 was done by Barrière et al., 2015), which were not available for this study.

385 In the flume experiments, the number of impulses recorded by each channel is strongly
386 correlated with sediment transport intensity for a wide degree of bedload transport rates.
387 Also, the lack of a decreasing trend in the number of impacts per second at the highest

388 transport rate seems to suggest that virtually all transported grains impacted on the
389 sensor even at the highest rates. During the flume experiments, grains were observed to
390 slide and roll over the pipe sensor, but also to jump over it. Indeed, the range of bedload
391 rate explored in the flume extends up to 453 g m^{-1} s^{-1}, which would correspond to high
392 transport rates during ordinary events, where both rolling and saltation of grains would
393 occur. For example, in the high-gradient Rio Cordon stream in the Eastern Italian Alps,
394 bedload transport during ordinary events reached 600 g m^{-1} s^{-1}, and only over short
395 periods during the extraordinary 1994 event raised up to 25000 g m^{-1} s^{-1}(Lenzi et al.,
396 2004). No sign of lower impacts registered at the highest transport rates isevident even
397 in the field, where the highest bedload intensity reached 1851 g m^{-1} s^{-1}. This would
398 suggest that, by protruding for few centimetres from the bed, the sensor is able to
399 capture sediments transported under different type of particle motion, even if flow
400 velocity and local flow field conditions could greatly influence the number of registered
401 impulses (i.e. Rickenmann et al., 2014).

402 Overall, the procedure for calibrating transport rates and grain size using the 6available
403 channels of the Japanese acoustic pipe seems robust and practical in flume experiments.
404 The method is based on the evidence that the intensities of impulses decrease
405 consistently from finer to coarser particles on each channel. This is comparable with
406 what obtained with the Swiss plate geophone system for particles coarser than about 30
407 to 40 mm (Rickenmann et al., 2014), for which less impulses per bedload mass are
408 recorded with increasing particle size. This is likely due to the fact that, for a given
409 bedload flux or bedload mass, there are fewer coarser than finer particles which may
410 potentially hit the plate or pipe.However, including field data into the calibration of
411 transport rates and grain size obtained using the 6 available channels proved
412 challenging, as the grain size of transported sediments is poorly predicted by the tested

413 empirical approaches. This is likely due to the fact that the grain size of transported
414 sediments is not strongly correlated with the transport rate (R = 0.42; Mao and
415 Carrillo,submitted). Similar trends are commonly observed in high-gradient stream and
416 have been related to equalmobility transport conditions for a wide range of particles
417 sizes (e.g. Marion andWeirich, 2003; Mao and Lenzi, 2007).The lack of a very strong
418 relationship between transport rates and transported sizes has been reportedalso by
419 Dell'Agnese et al. (2014), who incidentally found a good regression between the
420 transport rate and the number of impulses registered for the less sensitive channels of a
421 Japanese acoustic pipe. Indeed, by expressing their power-law regression between
422 transport rates and number of impulses registered for channel 6 as in Table 1, the
423 coefficient and exponent derived from the Saldur River are remarkably similar to what
424 we obtained for the Estero Morales, being for example the exponent 1.79 in the former
425 and 1.29 in the latter, respectively. In fact, Figure 8 shows that Dell'Agnese et al.
426 (2014) empirical regression using channel 6 would predict fairly well the bedload
427 transport rates of the Estero Morales, especially at the highest transport rates. This
428 suggests that only a few field observations with a new bedload monitoring station on a
429 high-gradient boulder stream could provide a good approximation for assessing bedload
430 transport rates simply using channel 5 or 6 of the acoustic pipe. On the other hand, a
431 deeper analysis using all channels as provided by an empirical equation like Eq. 1,
432 could provide insights on the size of transported sediments, which is a relevant
433 information river scientists and practitioners.

434 With future studies, raw data could be potentially used to assess the size of transported
435 particles in a more sophisticated way. For instance, Wyss et al. (2014) recently proved
436 that the amplitude of the signals captured by a Swiss geophone plate could be
437 successfullyused to extract grain size information from a geophone system. Wyss et al.

438 (in press) further extended this calibration demonstrating that the raw signal of Swiss
439 plate geophonescan be used to calculate impulse-based and packets-based (single
440 particle impacts) amplitude histogramsthat can be related with good confidence to grain
441 size classesand fractional bedload mass transport of particles coarser than 9.5 mm. In
442 the present study, with the Japanese acoustic pipe we used different channels which can
443 be considered amplification factors as pulses are generated using band-path filter with
444 predefined thresholds, thus are analogous to the packet counts for different amplitude
445 classes with the Swiss plate geophone system. Indeed, the calibration of a Japanese
446 acoustic pipe could be further improved by analysing the number and magnitude of raw
447 signals registered by the sensor. For example, Tsakaris et al. (2014) accounted for the
448 number and magnitude of the signal spikes produced by the particle impacts on a plate
449 geophone in order to discriminate rolling or saltation mode of transported particles.
450 Their results point out that discriminating the grain size from signals provided by a
451 geophone could be hampered by the fact that rolling and saltating particles may
452 generate responses at multiple acoustic frequencies over a wider spectrum.
453 Unfortunately, we could not record the raw data from the Japanese acoustic pipe and
454 could not perform similar analyses. However, Rickenmann et al. (2014) found a strong
455 correlation between the number of impulses registered by a Swiss plate geophone and a
456 series of other parameters derived from the raw signal of the geophone, suggesting that
457 the number of impacts is thus a good estimator of bedload transport rates of particles
458 with a minimum grain size of about 20 mm.

459 The impact plate used in this study registers the impacts in a single channel, and thus
460 does not allow to infer the grain size of the transported sediments. However, its use
461 seems very promising, as for each grain size used in the laboratory the transport rates
462 and impulses are strongly correlated. Also, the field-based regressions feature an

463 exponent remarkably similar to what obtained using the Japanese acoustic pipe.
464 However, the regression obtained in the Estero Morales is poor (R^2 = 0.16) and this
465 could be due to the fact that the plate is smaller than the pipe (150 *vs.* 500 mm) and does
466 not protrude into the flow, thus limiting the chance of monitoring saltating particles. On
467 the other hand, being longer than the diameter of the pipe (130 mm vs. 80 mm) the
468 plates allow capturing the impacts of saltating particles with longer hop lengths than for
469 the pipe. Overall, it seems that the Japaneseacoustic pipe and the impact plates,
470 especially the Swiss geophone plates which have been successfully calibrated in the
471 field (e.g. Rickenmann et al., 2014),provide different but complementary data that have
472 not been directly compared as yet, even if current efforts of producing devices with both
473 sensors are underway (John Laronne, personal communication). Indeed, an attempt of
474 comparing different indirect measuring systems is still lacking in literature, and this
475 reduces the chances of using calibration formulas in streams different than those on
476 which they have been tested.

477

478 ## 5. Conclusions

479 The Japanese acoustic pipe proved to be an inexpensive and robust device for
480 monitoring both the intensity and the grain size of coarse bedload transport in flume
481 experiments, as the six channels at which raw data are pre-processed could be used to
482 calibrate these two variables. The flume calibration appears to predict well the transport
483 of grains coarser than 9 mm, and could be confidently used on flume experiments when
484 detailed and continuous measurements of transported grain size is needed, for example
485 during unsteady-flow experiments, which are challenging but are becoming more
486 common practice recently (e.g. Waters and Curran, 2015). The impact plate with
487 accelerometer can also be calibrated to obtainreliable assessment of sediment transport

intensity. However, the grain size of the transported particles could not be calibrated in this study, so that the device would work well on flume experiments using homogeneous mixtures. Nonetheless, using row data provided by an advanced acoustic version of the impact plate, Wyss et al. (in press) were able to calibrate for bedload mass fluxes and grain sizes. When installed in a high-gradient mountain stream, the acoustic pipe could not be calibrated well for the grain size of transported material, mainly due to the fact that the transport conditions approached the equal mobility conditions for the range of explored discharges. However, despite of that the bedload intensity could be calibrated reasonably well. As previously reported by Dell'Agnese et al. (2014), Bunte-type nets proved to be reliableand flexible samplers for collecting bedload data to calibratesurrogate sensors. The impact plate could not be calibrated as well as the acoustic pipe in the field, but nonetheless allowed to detect the start and end, and the temporal dynamics of bedload transport. Further investigations using the raw data of these surrogate devices could allow enhanced and more detailed calibrations, as recently proved by Wyss et al. (in press) and Barrière et al. (2015) who could also extend the calibration of a wider range of grain sizes. This could provide reliable systems for river management agencies, looking for relatively cheap and reliable ways of monitoring continuously sediment transport in rivers.

Acknowledgments

The research was supported by the project FONDECYT 1130378. We are grateful to the Corporación Nacional Forestal (CONAF) for the interest and support in this study. We thank Joaquin Lobato, Fernanda Gordo, Riccardo Rainato, and Matteo Toro for their help in the laboratory and in the field.

References

Barrière, J., Krein, A., Oth, A., Schenkluhn, R., 2015. An advanced signal processing technique for deriving grain size information of bedload transport from impact plate vibration measurements. Earth Surf. Process. Landforms 40, 913–924. doi:10.1002/esp.3693.

Barry, J.J., Buffington, J.M., King, J.G., 2004. A general power equation for predicting bed load transport rates in gravel bed rivers. Water Resour. Res. 40, 2–3. doi:10.1029/2004WR003190.

Belleudy, P., Valette, A., Graff, B., 2010. Passive hydrophone monitoring of bedload in river beds: first trials of signal spectral analyses, U.S. Geological Survey Scientific Investigations Report 2010-5091.

Beylich, A.A., Laute, K., 2014. Combining impact sensor field and laboratory flume measurements with other techniques for studying fluvial bedload transport in steep mountain streams. Geomorphology 218, 72–87. doi:10.1016/j.geomorph.2013.09.004.

Bogen, J., Møen, K., 2003. Bed load measurements with a new passive acoustic sensor, in: Bogen, J., Fergus, T., Walling, D.E. (Eds.), Erosion and Sediment Transport Measurement in Rivers: Technological and Methodological Advances. IAHS Publication, 283. IAHS, Wallingford, pp. 181–192.

Bunte, K., Abt, S.R., 2005. Effect of sampling time on measured gravel bed load transport rates in a coarse-bedded stream. Water Resour. Res. 41, 1–12. doi:10.1029/2004WR003880.

Bunte, K., Abt, S.R., Potyondy, J.P., Ryan, S.E., 2004. Measurement of Coarse Gravel and Cobble Transport Using Portable Bedload Traps. J. Hydraul. Eng. 130, 879–893. doi:10.1061/(ASCE)0733-9429(2004)130:9(879).

Bunte, K., Swingle, K.W., Abt, S.R., 2007. Guidelines for using bedload traps in coarse-bedded mountain streams: construction, installation, operation and sample processing. US Department of Agriculture, Forest Service, Rocky Mountain Research Station.

Comiti, F., Mao, L., 2012. Recent Advances in the Dynamics of Steep Channels. In: Church, M., Biron, P.M., Roy, A.G. (Eds.), Gravel-Bed Rivers: Processes, Tools, Environments. John Wiley & Sons, Ltd, Chichester, UK, pp. 353-377.

D'agostino, V., Lenzi, M.A., 1999. Bedload transport in the instrumented catchment of the Rio Cordon. Part 1: Analysis of Bedload Records, Conditions and Threshold of Bedload Entrainment. Catena 36, 191–204.

Dell'Agnese, A., Mao, L., Comiti, F., 2014. Calibration of an acoustic pipe sensor through bedload traps in a glacierized basin. Catena 121, 222–231. doi:10.1016/j.catena.2014.05.021.

Emmett, W.W., 1980. A field calibration of the sediment trapping characteristics of the Helley-Smith bedload sampler, Geol. Survey Prof. Paper 1139. Washington, DC.

Geay, T., 2013. Mesure acoustique passive du transport par charriage dans les rivières. [Passive acoustic measurement of bedload transport in rivers]. Université Joseph Fourier, Grenoble, France.

Gray, J.R., Laronne, J.B., Marr, J.D.G., 2010. Bedload-surrogate monitoring technologies. U.S. Geological Survey Scientific Investigations Report 2010–5091, 37 p. also available at http://pubs.usgs.gov/sir/2010/5091.

Habersack, H.M., Nachtnebel, H.P., Laronne, J.B., 2001. The continuous measurement of bedload discharge in a large alpine gravel bed river. J. Hydraul. Res. 39, 125–133.

561 Hilldale, R., Carpenter, W., Goodwiller, B., Chambers, J., Randle, T., 2015.Installation
562 of Impact Plates to Continuously Measure Bed Load: Elwha River, Washington,
563 USA. J. Hydraul. Eng. 141(3), 06014023.
564 Infante Fabres, N.O., 2009. El Monumento natural El Morado (Andes Centrales
565 Chilenos). Análisis del medio biofísico, paisaje y propuestas para su gestión.
566 University of Barcelona, Spain.
567 Lenzi, M.A., 2004. Magnitude-frequency analysis of bed load data in an Alpine boulder
568 bed stream. Water Resour. Res. 40, W07201. doi:10.1029/2003WR002961.
569 Liébault, F., Laronne, J.B., 2008. Evaluation of bedload yield in gravel-bed rivers using
570 scour chains and painted tracers: the case of the Esconavette Torrent (Southern
571 French Prealps). Geodin. Acta 21, 23–34. doi:10.3166/ga.21.23-34.
572 Lucía, A., Recking, A., Martín-Duque, J.F., Storz-Peretz, Y., Laronne, J.B., 2013.
573 Continuous monitoring of bedload discharge in a small, steep sandy channel. J.
574 Hydrol. 497, 37–50. doi:10.1016/j.jhydrol.2013.05.034.
575 Mao, L., Dell'Agnese, A., Huincache, C., Penna, D., Engel, M., Niedrist, G., Comiti, F.,
576 2014. Bedload hysteresis in a glacier-fed mountain river. Earth Surf. Process.
577 Landforms 39(7), 964-976. doi:10.1002/esp.3563.
578 Mao, L., Lenzi, M.A., 2007. Sediment mobility and bedload transport conditions in an
579 alpine stream. Hydrol. Process. 21, 1882–1891. doi:10.1002/hyp.6372.
580 Mao, L., Carrillo, R., Spatial and temporal dynamics of suspended sediment transport in
581 a glacierized Andean basin. Submitted to Geomorphology.
582 Marion, D.A., Weirich, F., 2003. Eqal-mobility bed load transport in a small, step-pool
583 channel in the Ouachita Mountains. Geomorphology 55, 139–154.
584 doi:10.1016/S0169-555X(03)00137-5.
585 Mizuyama, T., Fujita, M., Nonaka, M., 2003. Measurement of bed load with the use of
586 hydrophones in mountain torrents, in: Bogen, J., Fergus, T., Walling, D.E. (Eds.),
587 Erosion and Sediment Transport Measurement in Rivers: Technological and
588 Methodological Advances. IAHS Publication, 283. IAHS, Wallingford, pp. 222–
589 227.
590 Mizuyama, T., Laronne, J.B., Nonaka, M., Sawada, T., Satofuka, Y., Matsuoka, M.,
591 Yamashita, S., Sako, Y., Tamaki, S., Watari, M., Yamaguchi, S., Tsuruta, K.,
592 2010a. Calibration of a passive acoustic bedload monitoring system in japanese
593 mountain rivers, U.S. Geological Survey Scientific Investigations Report 2010-
594 5091.
595 Mizuyama, T., Oda, A., Laronne, J.B., 2010b. Laboratory tests of a Japanese pipe
596 geophone for continuous acoustic monitoring of coarse bedload, U.S. Geological
597 Survey Scientific Investigations Report 2010-5091.
598 Recking, A., 2012. Influence of sediment supply on mountain streams bedload
599 transport. Geomorphology 175-176, 139–150.
600 doi:10.1016/j.geomorph.2012.07.005
601 Rennie, C.D., Church, M., 2010. Mapping spatial distributions and uncertainty of water
602 and sediment flux in a large gravel bed river reach using an acoustic Doppler
603 current profiler. J. Geophys. Res. 115, F03035. doi:10.1029/2009JF001556.
604 Richardson, K., Benson, I., Carling, P.A., 2003. An instrument to record sediment
605 movement in bedrock channels, in:Bogen, J., Fergus, T., Walling, D.E. (Eds.),
606 Erosion and Sediment Transport Measurement in Rivers: Technological and
607 Methodological Advances. IAHS Publication, 283. IAHS, Wallingford, Oslo,
608 Norway, 19-21 June 2002, pp. 228–235.

609 Rickenmann, D., McArdell, B.W., 2007. Continuous measurement of sediment
610 transport in the Erlenbach stream using piezoelectric bedload impact sensors. Earth
611 Surf. Process. Landforms 32, 1362–1378. doi:10.1002/esp.1478.
612 Rickenmann, D. Koschni, A., 2010. Sediment loads due to fluvial transport and debris
613 flows during the 2005 flood events in Switzerland. Hydrol. Process. 24, 993–1007.
614 doi: 10.1002/hyp.7536.
615 Rickenmann, D., Turowski, J.M., Fritschi, B., Klaiber, A., Ludwig, A., 2012. Bedload
616 transport measurements at the Erlenbach stream with geophones and automated
617 basket samplers. Earth Surf. Process. Landforms 37, 1000–1011.
618 doi:10.1002/esp.3225.
619 Rickenmann, D., Turowski, J.M., Fritschi, B., Wyss, C., Laronne, J., Barzilai, R., Reid,
620 I., Kreisler, A., Aigner, J., Seitz, H., Habersack, H., 2014. Bedload transport
621 measurements with impact plate geophones: Comparison of sensor calibration in
622 different gravel-bed streams. Earth Surf. Process. Landforms 39, 928–942.
623 doi:10.1002/esp.3499.
624 Tacconi, P., Billi, P., 1987. Bed load transport measurements by the vortex-tube trap on
625 Virginio Creek, Italy., in: Thorne, C.R., Bathurst, J.C., Hey, R.D. (Eds.), Sediment
626 Transfer in Gravel-Bed Rivers. John Wiley, Chichester, pp. 583–615.
627 Tsakiris, A., 2014. Signature of bedload particle transport mode in the acoustic signal of
628 a geophone. J. Hydraul. Research 52, 185-204.
629 doi:10.1080/00221686.2013.876454.
630 Turowski, J.M., Badoux, A., Rickenmann, D., 2011. Start and end of bedload transport
631 in gravel-bed streams. Geophys. Res. Lett. 38, L04401.
632 doi:10.1029/2010GL046558.
633 Vázquez-Tarrío, D., Menéndez-Duarte, R., 2015. Assessment of bedload equations
634 using data obtained with tracers in two coarse-bed mountain streams (Narcea River
635 basin, NW Spain). Geomorphology 238, 78–93.
636 doi:10.1016/j.geomorph.2015.02.032.
637 Vericat, D., Church, M., Batalla, R.J., 2006. Bed load bias: Comparison of
638 measurements obtained using two (76 and 152 mm) Helley-Smith samplers in a
639 gravel bed river. Water Resour. Res. 42, W01402. doi:10.1029/2005WR004025.
640 Waters, K.A., Curran, J.C., 2015. Linking bed morphology changes of two sediment
641 mixtures to sediment transport predictions in unsteady flows. Water Resour. Res.,
642 51(4), 2724-2741.
643 Wyss, C.R., Rickenmann, D., Fritschi, B., Turowski, J.M., Weitbrecht, V., Boes, R.M.,
644 2014. Bedload grain size estimation from the indirect monitoring of bedload
645 transport with Swiss plate geophones at the Erlenbach stream, in: Al., S. et (Ed.),
646 River Flow. Taylor & Francis Group, London, pp. 1907–1912.
647 Wyss, C.R., Rickenmann, D., Fritschi, B., Turowski, J.M., Weitbrecht, V., Boes, R.M.,.
648 Measuring bedload transport rates by grain-size fraction using the Swiss plate
649 geophone signal at the Erlenbach. Journal of Hydraulic Engineering, in press.
650

651

652 **TABLES**

653

654 **Table 1.** Coefficients, exponents, coefficients of determination, standard errors and p-
655 values for the power law regressions relating sediment transport intensity (q_s, g m^{-1} s^{-1})

656 and number of impulses (impulses m^{-1} s^{-1}) for each channel of the acoustic pipe and for
657 each sediment mixtures used in the laboratory and the data collected in the field.

Mixture	Ch.	a	b	Se (a)	Se (b)	R^2	p	Mixture	Ch.	a	b	Se (a)	Se (b)	R^2	p
WS	1	50.901	1.247	2.528	0.041	0.950	<0.001	PS	1	35.984	1.113	0.630	0.018	0.989	<0.001
35.9mm	2	90.811	1.121	2.860	0.033	0.958	<0.001	27.03mm	2	59.079	1.014	0.621	0.015	0.991	<0.001
	3	143.852	1.032	3.609	0.032	0.954	<0.001		3	91.397	0.970	1.042	0.018	0.986	<0.001
	4	208.687	1.025	4.964	0.032	0.955	<0.001		4	119.952	0.937	1.793	0.020	0.982	<0.001
	5	276.729	0.999	7.840	0.034	0.950	<0.001		5	143.634	0.935	2.568	0.021	0.982	<0.001
	6	349.742	1.009	10.216	0.030	0.959	<0.001		6	177.219	0.964	3.781	0.022	0.982	<0.001
WS	1	29.062	1.393	1.846	0.050	0.967	<0.001	PS	1	6.444	1.176	1.494	0.100	0.804	<0.001
24.6mm	2	40.602	1.277	1.907	0.040	0.972	<0.001	15.01mm	2	12.450	1.015	1.847	0.070	0.853	<0.001
	3	55.446	1.240	1.964	0.036	0.976	<0.001		3	21.891	0.935	1.848	0.046	0.907	<0.001
	4	79.342	1.155	2.149	0.034	0.975	<0.001		4	40.545	0.890	1.585	0.029	0.955	<0.001
	5	106.590	1.151	2.280	0.033	0.975	<0.001		5	80.628	0.985	1.392	0.025	0.974	<0.001
	6	170.976	1.217	3.744	0.042	0.966	<0.001		6	156.049	1.133	2.499	0.028	0.976	<0.001
WS	1	2.081	1.524	0.267	0.058	0.953	<0.001	PS	1	0.086	2.400	0.024	0.099	0.936	<0.001
13.0mm	2	5.259	1.194	0.385	0.036	0.971	<0.001	9.04mm	2	0.448	1.908	0.087	0.071	0.953	<0.001
	3	8.614	1.047	0.480	0.029	0.974	<0.001		3	2.092	1.553	0.220	0.044	0.972	<0.001
	4	12.551	1.009	0.594	0.029	0.973	<0.001		4	8.551	1.373	0.581	0.041	0.971	<0.001
	5	47.900	0.938	0.813	0.028	0.971	<0.001		5	63.975	1.173	1.384	0.051	0.941	<0.001
	6	179.467	0.816	10.796	0.038	0.933	<0.001		6	184.456	0.797	16.339	0.061	0.823	<0.001
WS	1	0.031	2.235	0.013	0.132	0.915	<0.001	EM	1	1186.04	-0.81	3605.8	1.179	0.084	>0.1
5.6mm	2	0.107	1.971	0.027	0.084	0.952	<0.001		2	0.013	3.948	0.034	1.027	0.373	>0.1
	3	4.767	0.977	0.767	0.075	0.890	<0.001		3	1.341	2.352	1.856	0.580	0.444	>0.1
	4	46.363	0.215	2.978	0.032	0.641	<0.001		4	5.013	2.168	4.281	0.394	0.509	>0.1
	5	287.574	0.385	337.566	0.219	0.641	>0.01		5	109.628	1.444	28.214	0.208	0.563	<0.001
	6	*							6	381.641	1.297	44.496	0.209	0.536	<0.001

658

659 **Table 2.** Summary of coefficients, exponents, coefficient of determination, and p-values
660 for the Eq. 1 fitted to obtain the D_{16}, D_{50}, and D_{84} using all well-sorted (WS) and
661 poorly-sorted (PS) mixtures, all flume data, data obtained in the Estero Morales (EM),
662 and the whole dataset. Numbers in bold are significant at $p < 0.01$.

Mixture	D_{xx}	a	b	c	d	e	R^2	*p*
WS	16	**22.692**	**0.607**	**-0.460**	**0.317**	**-0.463**	0.89	0.000
PS	16	**28.362**	**0.097**	-0.002	**-0.297**	**-0.290**	0.97	0.969
All flume	16	**28.893**	**0.357**	**-0.420**	0.109	**-0.471**	0.89	0.076
EM	16	**41.193**	-0.636	0.606	-0.430	-0.364	0.34	0.466
All flume and EM	16	**26.659**	**0.356**	**-0.456**	0.119	**-0.472**	0.84	0.099
WS	50	**29.259**	**0.492**	**-0.391**	**0.256**	**-0.418**	0.91	0.000
PS	50	**35.685**	**-0.022**	**0.108**	**-0.088**	**-0.325**	0.96	0.395
All flume	50	**33.762**	**0.215**	**-0.187**	**0.108**	**-0.396**	0.93	0.006
EM	50	**164.707**	**-1.480**	**1.413**	-0.695	-0.476	0.47	0.158
All flume and EM	50	**38.100**	**0.159**	**-0.401**	**0.366**	**-0.475**	0.65	0.006
WS	84	**34.773**	**0.464**	**-0.373**	**0.242**	**-0.402**	0.91	0.000
PS	84	44.954	-0.089	0.166	0.006	-0.357	0.94	0.903
All flume	84	39.604	0.185	-0.110	0.104	-0.359	0.92	0.013
EM	84	**159.115**	-0.334	0.404	-0.566	-0.059	0.45	0.785
All flume and EM	84	**47.149**	0.115	**-0.463**	**0.518**	**-0.453**	0.43	0.111

663 **Table 3.** Summary of coefficients, exponents, coefficient of determination, and p-values
664 for the Eq. 2 fitted to obtain the standard deviation of the transported sediment samples
665 using all well-sorted (WS) and poorly-sorted (PS) mixtures, all flume data, data
666 obtained in the Estero Morales (EM), and the whole dataset. Numbers in bold are
667 significant at $p < 0.01$.

Mixture	a	b	c	d	R^2	*p*
WS	**1.226**	**-0.043**	**0.026**	0.004	0.69	0.340
PS	**1.281**	**-0.105**	**0.261**	**-0.088**	0.65	0.000
All flume	**1.233**	**-0.059**	**0.142**	**-0.025**	0.58	0.024
EM	**2.748**	0.076	**-0.210**	0.103	0.28	0.182
All flume and EM	**1.307**	**-0.076**	**0.191**	-0.025	0.42	0.160

668

669 **Table 4**. Summary of coefficients, exponents, coefficient of determination, and p-values
670 for the Eq. 3 and Eq. 4 fitted to obtain the transport intensities using all well-sorted
671 (WS) and poorly-sorted (PS) mixtures, all flume data, data obtained in the Estero
672 Morales (EM), and the whole dataset. Equations are derived using both the observed
673 (O) or the predicted (P) D_{50} and σ from Eq. 1 and 2, respectively. Numbers in bold are
674 significant at $p < 0.01$. Equations identified with a star are those shown in Figure 6.

Mixture	Eq.	D_{50} and/or σ	a	b	c	d	e	R^2	*p*
WS	3	O	**0.007**	**2.672**	**0.871**	**0.343**	-	0.85	0.021
PS	3	O	**68.261**	**0.269**	**0.793**	**-0.960**	-	0.94	0.000
All flume*	3	O	1.264	1.445	0.872	-0.763	-	0.89	0.000
EM	3	O	0.455	**0.879**	**1.704**	-0.232	-	0.68	0.582
All flume and EM	3	O	**5.358**	**0.927**	**0.771**	**-0.562**	-	0.73	0.000
WS	3	P	**0.0003**	**3.741**	**1.305**	**0.088**	-	0.94	0.007
PS	3	P	**68.32**	**0.282**	**0.797**	**-0.989**	-	0.94	0.027
All flume*	3	P	**0.535**	**1.643**	**0.919**	**-0.617**	-	0.87	0.011
EM	3	P	1.5 E-4	**1.681**	**3.760**	-0.142	-	0.56	0.869
All flume and EM*	3	P	1.669	**1.312**	**1.323**	**-1.104**	-	0.61	0.420
WS	4	O	**3.5 E-8**	**5.092**	**1.079**	**0.665**	**20.335**	0.92	0.000
PS	4	O	**52.361**	**0.371**	**0.829**	**-0.896**	**-0.456**	0.94	0.001
All flume*	4	O	0.334	1.861	1.003	-0.403	-1.873	0.92	0.000
EM	4	O	0.275	**0.912**	**2.123**	0.008	**-1.197**	0.73	0.967
All flume and EM	4	O	**3.643**	**1.062**	**0.914**	**-0.436**	**-0.900**	0.75	0.000
WS	4	P	1.8 E-5	**4.172**	**1.323**	**0.168**	6.708	0.94	0.513
PS	4	P	**98.532**	**0.513**	**0.952**	**-0.421**	**-6.144**	0.95	0.013
All flume*	4	P	15.249	**1.174**	**0.999**	-0.117	**-9.390**	0.88	0.203
EM	4	P	**4.2 E-13**	**2.251**	**3.591**	**1.570**	**16.186**	0.57	0,000
All flume and EM*	4	P	236.61	**0.841**	**1.791**	0.379	**-15.716**	0.61	0.492

675

676 **Table 5.** Coefficients, exponents, coefficients of determination, standard errors and p-
677 values for the power law regressions relating sediment transport intensity (q_s, g m^{-1} s^{-1})
678 and number of impulses (impulses m^{-1} s^{-1}) registered by the impact plate and for each
679 sediment mixtures used in the laboratory and the data collected in the field.

Mixture	a	b	Se (a)	Se (b)	R^2	p
WS 35.9mm	30.829	1.097	2.044	0.037	0.893	<0.001
WS 24.6mm	11.315	1.249	1.076	0.043	0.922	<0.001
WS 13.0mm	1.305	1.416	0.543	0.164	0.669	<0.001
WS 5.6mm	7.201	0.747	0.614	0.036	0.871	<0.001
PS 27.03mm	26.195	0.974	0.919	0.026	0.974	<0.001

PS 15.01mm	4.477	1.294	0.744	0.068	0.824	<0.001
PS 9.04mm	0.255	2.015	0.104	0.146	0.790	<0.001
EM	7.226	1.230	7.398	0.381	0.157	>0.01

680

681 **FIGURE CAPTION**

682 **Figure 1.** Grain size distribution of the well sorted (WS) and poorly sorted (PS)
683 sediment mixtures used in the experiments. The names of the series on the legend
684 correspond to the D_{50} of the mixtures.

685 **Figure 2**. Picture of the impact plates and the acoustic pipe installed in the flume (on
686 the left), and the monitored cross section where bedload sampling were collected in the
687 Estero Morales using Bunte-traps (on the right).

688 **Figure 3.** Relationship between transport intensity and number of impulses registered
689 by the Japanese acoustic pipe on each channel for each sediment mixtures used in the
690 laboratory and the data collected in the Estero Morales.

691 **Figure 4.** Relationships between intensities of impulses registered by channels of
692 different sensitivity by the Japanese acoustic pipe. The dotted line represents the
693 identity line.

694 **Figure 5.** Prediction of median grain size of transported sediments using data acquired
695 in the flume using well-sorted sediments (a) and poorly-sorted sediments (b), data
696 collected in the field (c), and the whole dataset (d) using the Japanese acoustic pipe. The
697 dotted line represents the identity line.

698 **Figure 6.** Observed *vs.*predicted values of bedload transport rates obtained using Eq. 3
699 (graphs on the left) or Eq. 4 (graphs on the right), and using observed (a and b) or
700 predicted (c and d) values of grain sizeusing the Japanese acoustic pipe. Graphs e and f
701 refer to equations derived using the whole of data collected in the field and in the flume.
702 The dotted line represents the identity line.

703 **Figure 7.** Relationship between transport intensity and number of impulses registered
704 by the impact plate for each sediment mixture used in the laboratory and the data
705 collected in the Estero Morales.

706 **Figure 8.**Observed *vs.*predicted values of bedload transport rates obtained using Eq. 4
707 (as in Figure 6f) and power-law regression proposed by Dell'Agnese et al. (2014) based
708 on field calibrationof a Japanese acoustic pipe.The dotted line represents the identity
709 line.

Figure (Color)

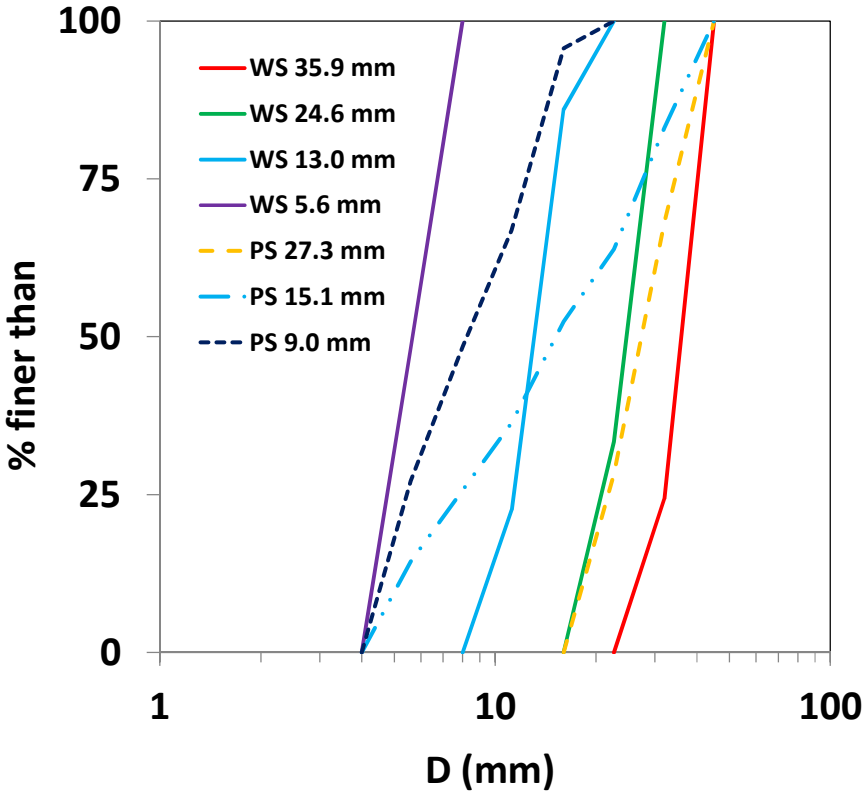

Figure (Color)

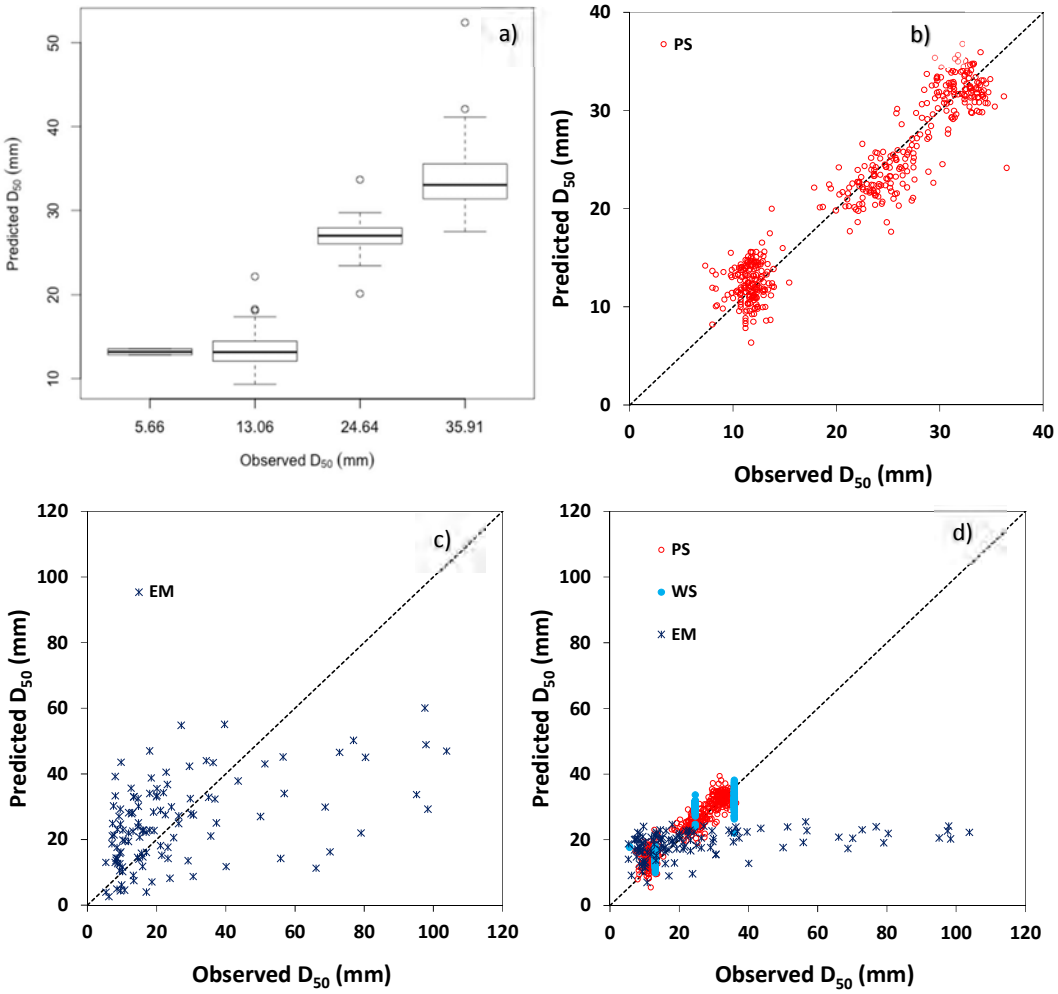

Figure (Color)